



## VALIDATION OF A 3D VELOCITY MODEL OF THE PUGET SOUND REGION BASED ON MODELING LONG PERIOD GROUND MOTION DATA

Arben PITARKA<sup>1</sup> Robert GRAVES<sup>2</sup> and Paul SOMERVILLE<sup>3</sup>

### SUMMARY

In this study we prepared a 3D velocity model suitable for modeling long-period wave propagation in the Puget Sound region. The model is based on products of SHIPS (Seismic Hazard Investigation in Puget Sound) and geophysical information from other studies of the region. The adequacy of the velocity model was evaluated based on analyses of goodness of fit between recorded and simulated ground motion velocity from the M6.8 Nisqually earthquake. The earthquake was located about 60 km south of Seattle with a hypocentral depth of 59 km. The analyses were performed in the frequency range of 0.02-0.5 Hz using data from 40 stations. Although our model covers a wide area of the Puget Sound region its quality is assessed in the Seattle region in which the distribution of stations that recorded the Nisqually earthquake was denser. Our 3D finite-difference ground motion modeling suggests that the propagation of long-period waves (periods longer than 3 s) in the Seattle basin is mostly affected by the deep basin structure. The tomographic velocity model of Parsons et al. [1] combined with the model of depth to the basement of the Seattle basin of Blakely [2] were essential in preparing and constraining geometrical features of the proposed velocity model.

### INTRODUCTION

Important advances have been made in recent years regarding our understanding of the deep and shallow crustal structure in the Puget Sound region, and its influence on the ground shaking from recorded earthquakes and other seismic sources. Much of the knowledge has arisen from the SHIPS experiments (e.g. Brocher et al. [3]; Brocher et al. [4]; Parsons et al. [1]; Calvert and Fisher [5]; Wagoner et al. [6]) and ground motion analyses and modeling (e.g. Frankel and Stephenson [7]; Frankel et al. [8]; Hartzell et al. [9]; Frankel et al. [10]; Pratt et al. [11]). Based on the SHIPS data many comprehensive studies of the underground structure have provided valuable information that can improve the quality of existing crustal

---

<sup>1</sup> Senior Project Scientist, URS Corporation, Pasadena, CA, USA. Email: arben\_pitarka@urscorp.com

<sup>2</sup> Principal Scientist, URS Corporation, Pasadena, CA, USA. Email: robert\_graves@urscorp.com

<sup>3</sup> Principal Scientist, URS Corporation, Pasadena, CA, USA. Email: paul\_somerville@urscorp.com

velocity models that are used in strong ground motion modeling and prediction in the Puget Sound metropolitan regions. The interpretation of refraction survey data (e.g. Brocher et al. [3]; Brocher et al. [4]) and high-resolution tomographic models of the Seattle basin have provided new information about the geometry of the southern edge of the basin, and structure of the sedimentary layers. (e.g. Calvert and Fisher [5]).

Investigations of geological structure in the Puget Sound metropolitan regions indicate the presence of strong lateral variations in the near surface geology (e.g. Finn et al. [12]; Johnson et al. [13]; Pratt et al. [14]; Brocher et al. [4]; Calvert and Fisher [5]). These basin structures have the potential to significantly increase the amplitude and duration of strong ground motions. Amplified ground motion with increased duration could cause significant damage to the built environment in the Seattle area, even during moderate earthquakes. This is demonstrated by the magnitude 6.8 February 28, 2001 Nisqually earthquake, which caused \$2 billion in damage. Development of 3D velocity models capable of accurately reproducing the effects of deep and shallow geology on ground motions from faults within the Puget Sound metropolitan regions is therefore an important task for seismic hazard assessment. The work presented here describes our effort to develop a 3D velocity model of the Puget Sound region that incorporates recent information on the structure of the crust, especially in the Seattle region. We discuss the details of the model parameterization and show results of the model validation analyses using recorded ground motion from the 2001 Nisqually earthquake.

## VELOCITY MODEL PARAMETERIZATION

The extensive SHIPS geophysical experiment, as well as other high resolution surveys, have helped to better characterize the crustal architecture and basin geometry, and map the sediment thickness and location of fault zones in the Puget Sound region. Tomographic velocity models of the Puget Sound region (e.g. Parsons et al. [1]; Brocher et al. [4]; Crosson et al. [15]; Wagoner et al.[6]) are characterized by marked lateral variation of the velocity in the crust, and the existence of deep basin structures. In order to provide accurate information on the effects of these underground structure complexities on the ground motion from earthquakes in the region, we need to progressively improve our velocity models by modeling more ground motion data as they become available, and extend the modeling capability to high frequencies. The analysis of modeling presented here is a part of such efforts.

Based on results of some of the SHIPS investigations we produced a 3D velocity model for an area that includes parts of the Puget Sound region. The location of the area covered by our model, and ground motion recording stations used in this study are shown in Figure 1. Our velocity model occupies a volume of 61kmx82kmx62km, and is characterized by three main components: 1) the background 3D crustal structure, 2) the basement and sedimentary layers of the Seattle basin, and 3) the thickness of the unconsolidated deposits throughout the region. The

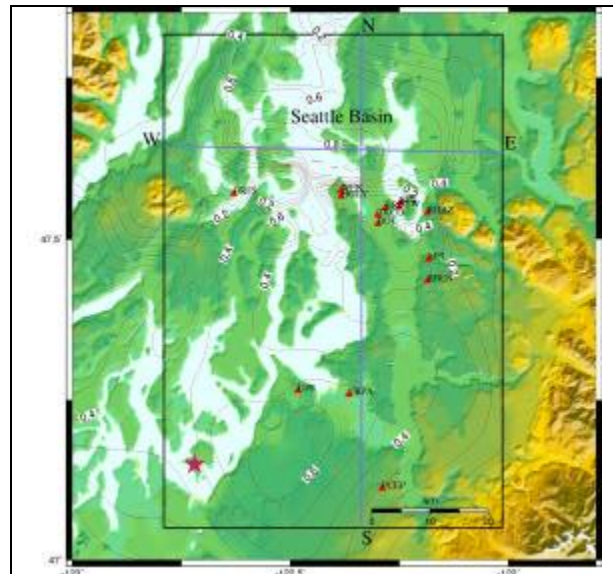


**Figure 1a. Map of the Puget Sound area.**

**Black rectangle delineates the area covered by the 3D velocity model. Blue lines indicate the location of N-S and EW vertical cross-sections of the model. Red triangles show the location of the strong motion station, and red star shows the epicenter location of the Nisqually earthquake. The red contours represent the depth to base of unconsolidated deposits.**

3D tomographic P-wave velocity crustal model of Parson et al. [1] was used to generate the background velocity of our model that reaches a depth of 62 km. The Parson et al. [1] model was obtained by inverting combined dense seismic reflection travel times and gravity anomaly data. The model gives the P-wave velocity on a regular grid with constant spacing of 1km. We resampled it on a finer grid with variable vertical spacing. The velocity at each point of the refined grid was calculated by linearly interpolating the velocity corresponding to the eight closest grid points of the original grid. The S-wave velocities in our model were derived from the P-wave velocities using the  $V_p/V_s$  ratio. Following Frankel and Stephenson [7] the  $V_p/V_s$  ratio was assumed to be 2.2 and 1.75 at depths above 2.5 km and below 2.5 km, respectively, while the density increases from 2.3 gm/cm<sup>3</sup> to 2.7 gm/cm<sup>3</sup>. Another velocity model parameter used in our wave-propagation finite-difference modeling method is the anelastic attenuation, which is represented by the Q factor. The implementation of the attenuation into our finite-difference method is based on the Graves [16] technique, which considers Q to be the same for both P- and S-waves, and frequency independent. Because of lack of reliable information on the anelastic attenuation in the considered region, we assumed Q to be 100 and 500 at depths smaller and greater than 2.5 km, respectively, except for the unconsolidated deposits where Q was assumed to be 50.

The part of the model that includes the Seattle basin to a depth of 10 km was prepared using combined data from the depth to basement map of Blakely [2] and a N-S cross-section of the Seattle basin sediments based on the interpretation of seismic reflection profiles during the SHIPS experiment (Brocher et al. [4]). This velocity profile as well as a high-resolution tomographic model of the area suggest that the southern edge of the Seattle basin dips toward the south. This important feature of the southern edge of the basin was not resolved by the gravimetric and aeromagnetic data used by Blakely [2], and is therefore not present in his depth to basin basement model. The profile, that extends to more than 10 km in depth, suggests that the basin sediments below 1 km consist of at least four distinctive layers with strong velocity contrast. In our model the profile was used to derive the geometry of the southern edge of the Seattle basin and the decreasing thickness of the sedimentary layers toward the north. The lateral variation of the layers thickness was assumed to be proportional to the corresponding basin depth and its N-S variation was assumed to be similar to that in the N-S velocity profile (see Figure 2). This procedure produces a basin velocity model that is in agreement with a 2D velocity model along an E-W cross section of the basin proposed by Miller and Snelson [17]. Their model indicates that the geometry of the boundaries between the sedimentary layers is similar to that of the basin basement. The assumed seismic parameters of the sedimentary layers are given in Table 1.

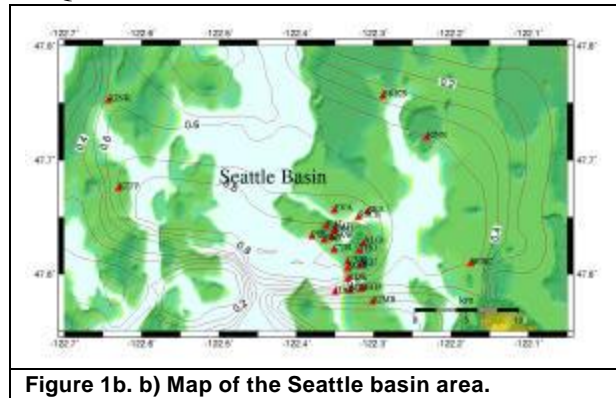


Figure 1b. b) Map of the Seattle basin area.

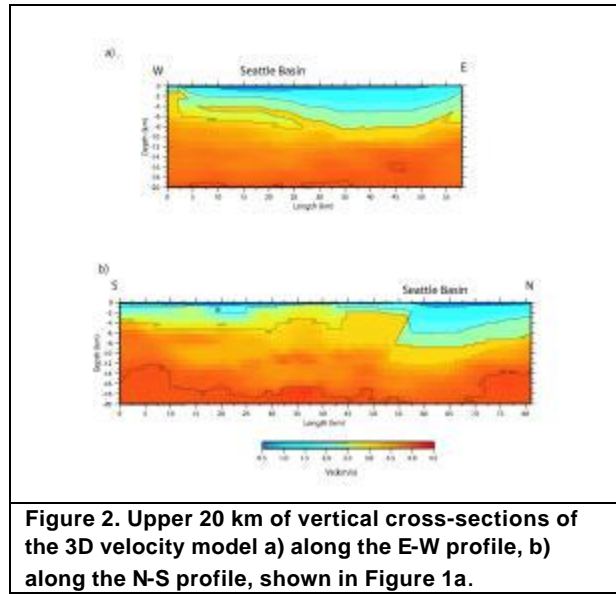


Figure 2. Upper 20 km of vertical cross-sections of the 3D velocity model a) along the E-W profile, b) along the N-S profile, shown in Figure 1a.

Besides the Seattle basin structure, a key feature in our velocity model is the thickness of the layer representing the unconsolidated deposits which consist mainly of Quaternary and possibly Pliocene deposits. The thickness of the unconsolidated deposits is well resolved only in the Seattle region where the surface deposits consist of Quaternary sediments (Johnson et al. [13]). In the other areas of the Seattle region our knowledge of the thickness of such deposits is poor. In our model it was derived from the maps of depth to basement of Yount et al. [18] and Hall and Othberg [19] for the northern part and the southern part of the Puget Sound region, respectively. These maps are based on geotechnical investigations using extrapolations between data that are sparsely distributed. In the velocity model we tested, the minimum grid spacing is 200 m. Consequently, the unconsolidated deposits are represented by a single layer with a minimum shear-wave velocity of 0.6 km/s. For this layer we assumed  $V_p = 1.5$  km/s, density = 2.1 g/cm<sup>3</sup> and  $Q=50$ .

**Table 1.** Velocity Model of the Seattle Basin Sediments

Layer	$V_p$ (km/sec)	$V_s$ (km/sec)	Density (g/cm <sup>3</sup> )	Q
Quaternary	1.5	0.6	2.1	50
1	1.8	1.2	2.2	50
2	2.7	1.6	2.4	50
3	3.3	1.9	2.6	250
4	4.0	2.3	2.7	300
5	5.3	3.1	2.8	400

Vertical cross sections of the 3D velocity model up to a depth of 20 km, and oriented in the E-W and N-S directions across the Seattle basin, are shown in Figures 2a and 2b, respectively. The location of the profiles is indicated by blue lines in Figure 1a. The strong discontinuity in the geological structure caused by the Seattle fault creates a zone of velocity contrast along the southern edge of the Seattle basin. The velocity contrast between the basement and the basin sediments, and the geometry of the basin edge in this area are key features of the basin structure that generate secondary basin waves. The velocity structure below 20km depth is very simple consisting mainly of very small vertical variations in the velocity. The shear wave velocity gradually increases from 4 km/s to 4.57 km/s in the depth interval of 20km-62 km. This structure is consistent with the results from a recent study which shows clear evidence that the region considered here is underlain by a low-velocity, serpentinized upper mantle (Brocher et al. [20]). The reduction of the velocity contrast in the Moho boundary caused by the low velocity in the upper mantle has significant effects in ground motions from deep earthquakes such as the Nisqually earthquake, and may reduce the amplitude and duration of the ground motion.

Our model shares some similarities and dissimilarities with another velocity model of the Seattle basin area proposed by Frankel and Stephenson [7]. Both velocity models use the same depth to the basin basement and Quaternary layer data. The main differences are in the way the basin sedimentary layers are represented, the geometry and the dip angle of the southern edge of the basin, and background regional velocity model.

## **MODELING GROUND MOTION FROM THE 2001 NISQUALLY EARTHQUAKE**

As a first step in the process of testing the velocity model, we computed long-period ground motion (2-10 sec) for the February 28, 2001 Nisqually earthquake ( $M=6.8$ ) and compared the synthetic and recorded velocity seismograms at 40 strong motion recording sites. The hypocenter was located at  $-122.4E$  and

32.5N and a depth of 59 km (Ichinose et al. [21]). The earthquake was recorded by strong ground motion stations operated by the United States Geological Survey and University of Washington. Because the earthquake source was relatively deep, most of the ground motion recorded at basin sites was dominated by the direct shear waves and basin generated secondary waves. The simulation was performed using the finite-difference method of Pitarka [22] using a regular grid with variable spacing in the vertical direction. The minimum grid spacing of 200 m, and its vertical variation insured accurate calculations of the wave-field up to a frequency of 0.5 Hz. The earthquake source was modeled by two double couple point sources separated in time by 1.5 s. Our source model was derived from the slip model obtained by Ichinose et al. [21] based on the inversion of ground motion and teleseismic data. The source model used in the finite-difference simulation is described in Table 2. The source time function for each point source was assumed to be of triangular shape.

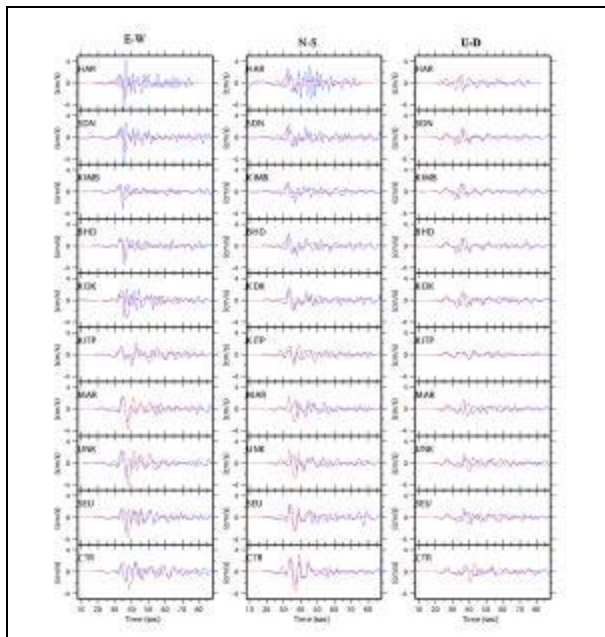


**Figure 3. Comparison of recorded (blue) with synthetic (red) velocity seismograms at sites in the Seattle basin.**

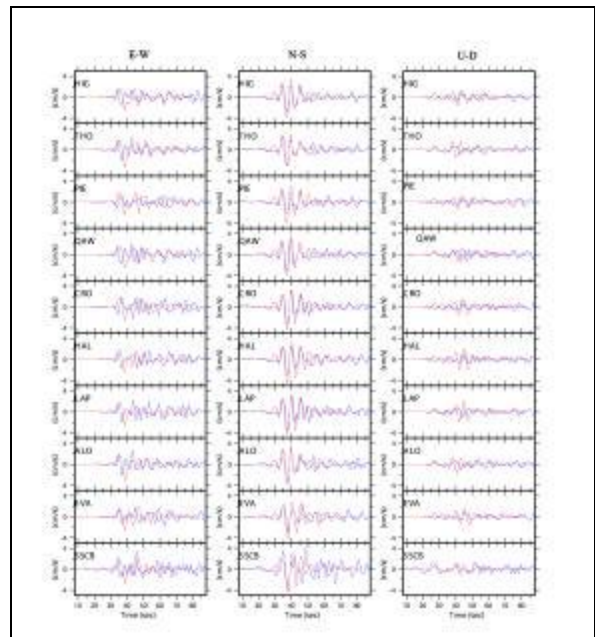


**Figure3. Continued**

The comparison between the synthetic and recorded velocity seismograms at sites inside and outside the Seattle basin, starting with the station closest to the epicenter, is shown in Figures 3 and 4, respectively. Both synthetic and recorded data are band-pass filtered at 0.1-0.5 Hz. The model does a good job at reproducing the phases carrying most of the seismic energy, and the duration of the ground motion at the Seattle basin sites. At sites HAR, SDN KIMB, BHD, and KDK, which are located near the southern edge of the basin, the waveform fit is less satisfactory. At these sites scattered waves with periods shorter than 3 sec are less developed in the synthetic seismograms. Such waves consist of reverberations of waves trapped within the surface layers.

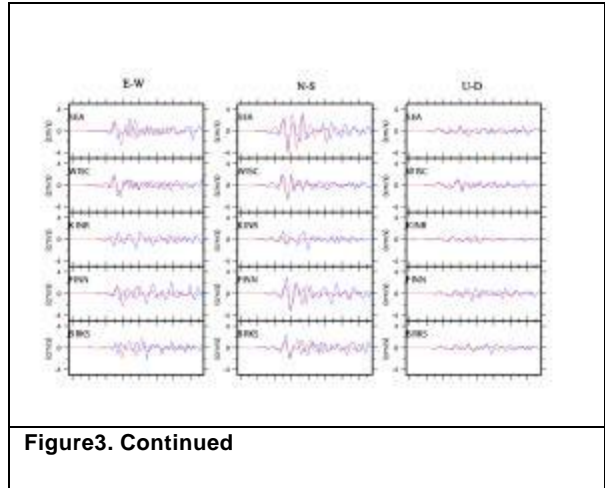


**Figure3. Continued**

The discrepancy may be related to the minimum shear-wave velocity of 600 m/s imposed to our model, which may alter wave propagation effects within the surface layers. It is also possible that the absence of high frequency waves in the synthetics is caused by the lack of high frequency variation in our slip velocity function which has spectral holes around 22.5 sec. At sites located in the central part of the basin and near the Ship Canal (e.g. CTR, HIG, THO, QAW, ALO, EVA, and SEA) the waveform fit is relatively good. At these sites the ground motion is characterized by two long period pulses followed by others with smaller amplitude. The first large pulse is the direct S-wave. The other large pulse following the first one is a basin basement reflected wave, mainly polarized in the vertical plane. Its amplitude remains significant even at stations FINN and BRKS where the shallow sedimentary layers become thinner, but the basement is still deep. Our simulation reproduces both pulses very well. A third phase followed by coda waves can be clearly seen in the E-W component of ground motion recorded at stations SEU, THO, PIE, QAW, CRO, HAL, ALO, EVA, and SSCB, which are located north of the southern edge of the basin. At these sites this phase arrives at least 15 sec after the direct S-wave. Its amplitude is comparable or even larger than that of the direct S-wave, and the delay time increases from south to north. As will be seen in maps of simulated peak velocity distribution this phase dominates the peak velocity at sites around Ship Canal in the central part of the basin.

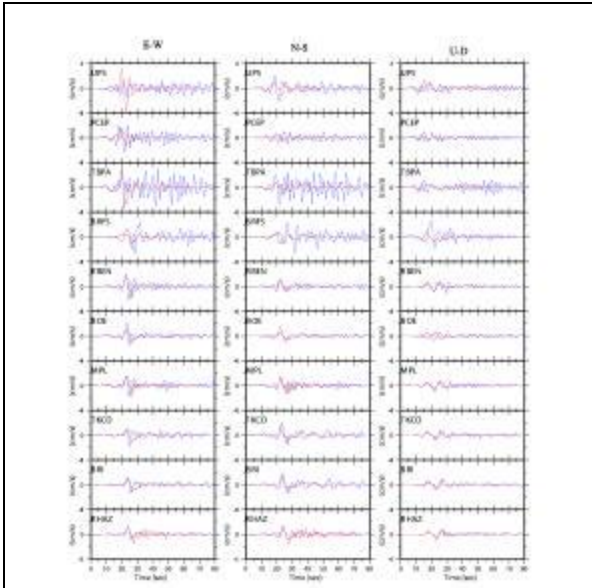


**Figure 4. Comparison of recorded (blue) with synthetic (red) velocity seismograms at sites outside the Seattle basin**

component than in the N-S component (see recorded motion at BHD, KDK, MAR, UNK, SEU, QAW, CRO, ALO, EVA, and SEA shown in Figure 3).

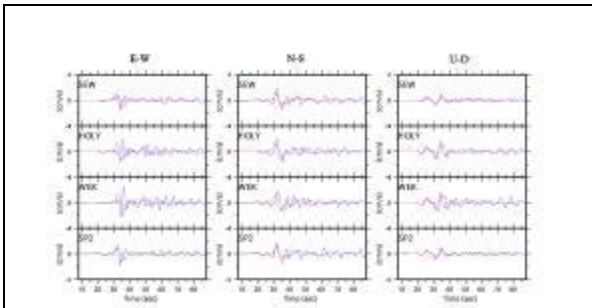


**Figure 4. Continued**

At sites outside the basin the waveform fit between the recorded and simulated seismograms is good except for UPS, PCEP, and BRF5 which are located in the southern part of the model in a deep basin. At these stations most of the seismic energy is carried by coda waves with periods between 2-3 sec. The simulation reproduces only the first part of the seismograms. The extremely long duration of the recorded coda waves and their relatively high frequency content, not reproduced by our model, indicate that the large basin structure in the southern part of the considered region is much more complex than the one in our model.

At sites in the southern and central parts of the Seattle basin, the travel time of the recorded largest pulse associated with the direct shear wave is shorter by at least 2.s in the E-W component than in the N-S component (see recorded motion at BHD, KDK, MAR, UNK, SEU, QAW, CRO, ALO, EVA, and SEA shown in Figure 3). This phenomenon is not observed at sites outside the basin. The fact that this time delay is not reproduced by our model, in which the soil is considered as isotropic (compare the synthetic and observed seismograms at stations mentioned above), suggests that there is anisotropy in the soil properties in the regions around the southern edge of the basin. This indicates that the Tertiary sedimentary rocks of the Seattle fault zone are highly fractured.

### GOODNESS OF FIT BETWEEN OBSERVED AND SIMULATED GROUND MOTION

In order to evaluate the quality of our velocity model, we analyzed the goodness of fit between simulated and recorded ground motion. Goodness-of-fit factors were derived for different ground motion parameters such as peak velocity and Fourier amplitude spectra in a given frequency range. The goodness-of-fit factor  $f_1$  corresponding to a ground motion parameter is given by (John Anderson, 2003, personal communication):

$$f_1 = \exp\left[-\left(\frac{Syn - Obs}{\min(Syn, Obs)}\right)^2\right]$$

where Obs and Syn are measures of the ground motion parameter using observed and synthetic seismograms, respectively, and  $\min(\text{Syn}, \text{Obs})$  is the smaller of the two.  $f_1$  varies from 0 to 1, with 1 corresponding to identical observed and simulated ground motion measures. In this study we calculated  $f_1$  using the peak ground velocity (PGV) of seismograms band-pass filtered at three different frequency ranges of 0.05-0.2 Hz, 0.05-0.3 Hz and 0.05-0.5 Hz, respectively, and Fourier Spectra Amplitude (FSA) averaged over a narrow band of 0.1 Hz centered at 0.2, 0.3 and 0.4 Hz.

In addition to  $f_1$  we calculated factor  $f_2$  which is given by the following formula:

$$f_2 = 2 \frac{\int p(t)_{obs} p(t)_{syn} dt}{\int p(t)_{obs}^2 dt + \int p(t)_{syn}^2 dt}$$

where  $p(t)_{obs}$  and  $p(t)_{syn}$  are the observed and synthetic seismograms, respectively. If the synthetic seismogram is null then  $f_2=0$ , and if the synthetic and observed seismograms are perfectly matched then  $f_2=1$ .  $f_2$  was calculated using a time window of 60 sec starting several seconds before the P-wave arrival time. Estimates of both factors in different frequency ranges provide a quantitative measure of the goodness of fit. Combined with the waveform comparison, they give a general picture of the waveform fit between the observed and synthetic ground motions. Variations of the  $f_1$  and  $f_2$  factors with epicentral distance for different frequency ranges are given in Figure 5.

The  $f_1$  values for PGV are shown in Figure 5a. The  $f_1$  values suggest that, except for a few sites, our velocity model does a very good job at predicting the peak velocity at sites in and outside the Seattle basin, for all three considered frequency ranges.

The  $f_1$  for the FSA is relatively high at 0.2 Hz (periods of 5 s) while it decreases substantially at frequencies 0.3 and 0.4 Hz, for which the signal energy is small (Figure 5b). Since most of the energy of the ground motion velocity is carried by waves with predominant period around 5 sec and longer, as seen in the waveforms shown in Figures 3 and 4, the value of  $f_1$  at 0.2 Hz is a good representation of the model quality.

Compared to  $f_1$  the goodness-of-fit factor  $f_2$  is much more sensitive to the waveform than the amplitude of the motion. Consequently it can reach values that are much smaller than the  $f_1$  factor for the same sites. The variation of  $f_2$ , shown in Figure 5c, suggests that at many sites, where the synthetic and recorded

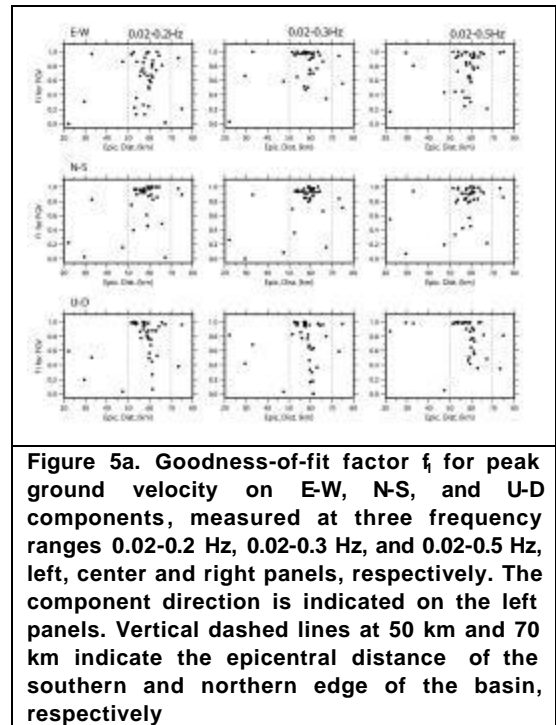


**Figure 5a. Goodness-of-fit factor  $f_1$  for peak ground velocity on E-W, N-S, and U-D components, measured at three frequency ranges 0.02-0.2 Hz, 0.02-0.3 Hz, and 0.02-0.5 Hz, left, center and right panels, respectively. The component direction is indicated on the left panels. Vertical dashed lines at 50 km and 70 km indicate the epicentral distance of the southern and northern edge of the basin, respectively**

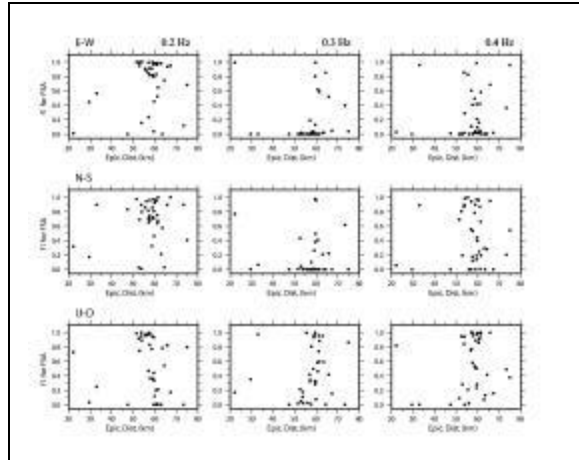


**Figure 5b. Goodness-of-fit factor  $f_1$  for Fourier amplitude spectrum of the velocity calculated at 0.2 Hz, 0.3 Hz, and 0.4 Hz, left, center and right panels, respectively for the EW, N-S, and U-D components. The components orientation is indicated on the left panels.**

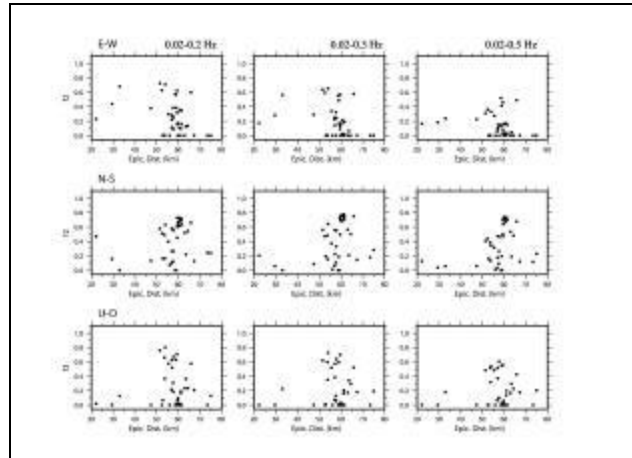


**Figure 5c. Goodness-of-fit factor  $f_2$  for velocity ground motion seismograms for the E-W, N-S, and U-D components, band-pass filtered at three frequency bands 0.02-0.2 Hz, 0.02-0.3 Hz, and 0.02-0.5 Hz, left, center and right panels, respectively.**

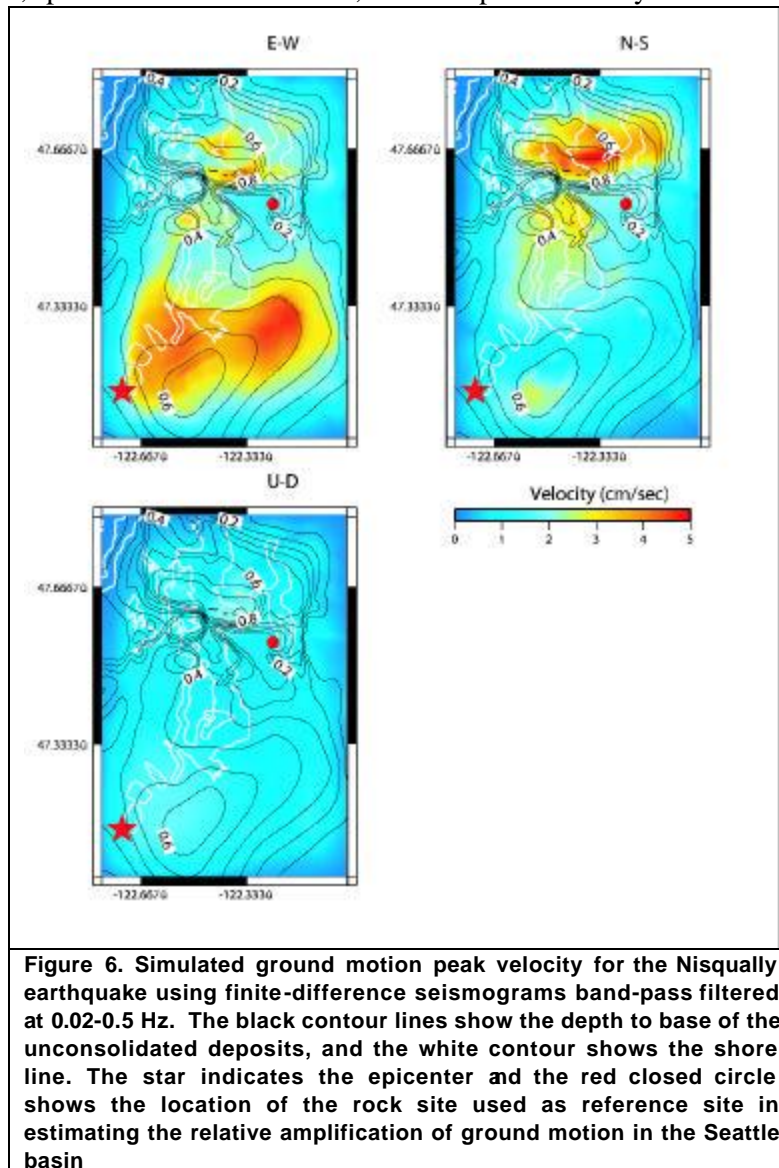
seismograms are not in phase, this factor could be as low as 0.1. Meanwhile at these sites  $f_1$  could be high. Our model performs reasonably well at matching the N-S and vertical components of motion at most of the sites in the Seattle basin (sites with epicentral distance between 52 and 65 km). At sites outside the basin  $f_2$  is low. At these sites we match well the amplitude and duration, but not the waveform of the ground motion.

The goodness of fit results demonstrate that in general the large-scale basin structure along the southern edge of the Seattle basin is well represented in our model. Overall, the best fit, in terms of waveform and amplitude, is obtained in the N-S component of the ground motion velocity, especially at sites located in the central part of the basin and with epicentral distance ranging between 52 and 65 km. At these sites the ground motion is dominated by large pulses, corresponding to the direct S-wave, basin reflected waves, and basin surface waves generated at the southern edge of the basin.

## DISCUSSION

Figure 6 shows the distribution of calculated peak ground velocity in the E-W, N-S and vertical components of motion. In this figure we also show contour lines of the unconsolidated sedimentary layer thickness. The peak velocity distribution indicates that the peak velocity amplification pattern is very complex, and it does not fully coincide with the unconsolidated sedimentary layer thickness, especially in the Seattle basin. In the Seattle basin the peak velocity amplification is very different between the two horizontal components. The E-W component of the ground motion is strongly amplified only along the southern edge, and in a small area of the central part of the basin, whereas the zone of amplification of the N-S component covers a large portion of the basin, off-set from the southern basin edge. In general the lateral extension of these zones of peak velocity amplification correlate with basins and the thickness of the unconsolidated deposits. This indicates that the long period waves are affected by the deep and shallow geological structure of the basin as well.

Based on the peak velocity distribution, there is striking evidence of very large amplification of the ground motion in the N-S direction in both Seattle and Tacoma basins. In the Seattle basin the N-S component is dominated by basin surface waves generated at the southern edge of the basin along a zone of strong velocity contrast. The N-S component, which roughly corresponds to the radial component of motion, may also contain Rayleigh waves that were generated in the Tacoma basin and then channeled through the Seattle uplift into the Seattle basin without being scattered (e.g. Pitarka and Irikura, [23]). Our simulation suggests that the amplification pattern is due to the 3D basin focusing and basin-edge effects. The surface waves remain trapped within the basin sediments. Their constructive superposition may create complex amplification patterns, even at long periods. As discussed earlier, the secondary surface waves in the Seattle basin may have been amplified due to the thinning of the sedimentary layers toward the north. This structural effect, specific to the Seattle basin, has been pointed out by Frankel and Stephenson [7].



Two recent site response studies in the Seattle region (Frankel et al. [8]; Hartzell et al. [9]) have identified several areas of high amplification in the Seattle basin. These findings, which are based on analyses of ground motion data at frequencies higher than the ones considered in our study, suggest that the high

amplification is due to several factors such as 3D basin-edge effects, basin focussing effects and higher impedance contrast between the basin sediments and the bedrock. Our modeling results suggest that the 3D basin structure has a strong effect at long periods.

In order to supplement the analysis of our 3D model quality in the Seattle region, we calculated the basin amplification at a linear station array across the Seattle basin (line E-W in Figure 1a) using simulated ground motion from the Nisqually earthquake. We compared it with the amplification estimated by Pratt et al. [11] using ground motion recordings of the Chi-chi, Taiwan earthquake. The location of our station array is very close to that of the 1999

SHIPS array that was used by Pratt et al. [11] in their study of the amplification of the seismic waves in the Seattle basin. The first and last stations of our array correspond to stations 1296 and 2570 in their study, respectively. Our stations are equally spaced at 400 m. Following the procedure used by Pratt et al. [11], we estimated the basin amplification at 0.2 Hz and 0.33 Hz by calculating the spectral ratios of the simulated horizontal motion from the Nisqually earthquake relative to a bedrock site. Pratt et al. (2003) estimated the basin amplification based on the average of spectral ratios of the recordings of the horizontal motion from Chi-chi, Taiwan earthquake relative to the average of two bedrock sites at the west end of the array in the Olympic Mountains. Because these two sites are located outside our 3D model area, we choose a site at -122.25 E, 47.549 N as a reference (see Figure 6) Based on recordings of the Chi-chi earthquake, Pratt et al. (2003) estimated that the site response relative to the Seward Park reference site will be at least about 30% smaller than the site response relative to the Olympic Mountains reference site that was used in their study. We reduced their amplification factors by 30% in order to obtain the corresponding amplification relative to the Seward Park reference site used in our calculation.

The comparison between the two amplifications at 0.2 Hz and 0.33 Hz relative to the Seward Park reference site is shown in Figure 7. The variation of the basin amplification factor along the considered E-W array is very similar between the two studies. Basically its shape is similar to the basin basement geometry. Our simulated amplification tends to be larger in the central part of the basin, and smaller in the western part of the basin. Although generated by a deep source, the simulated long-period ground motion from the Nisqually earthquake is affected by the radiation pattern. This is not the case for the recorded teleseismic ground motion from the Chi-chi earthquake. Given the completely different nature of the earthquake sources, the similarity between the two basin amplification factors is very encouraging. It demonstrates that the overall long-scale basin structure features along the E-W direction are adequately presented in the model. Seismological constraints based on modeling of amplification factors derived from recordings of local and regional earthquakes in the Puget Sound region will be very helpful in future refinements of proposed 3D velocity models.

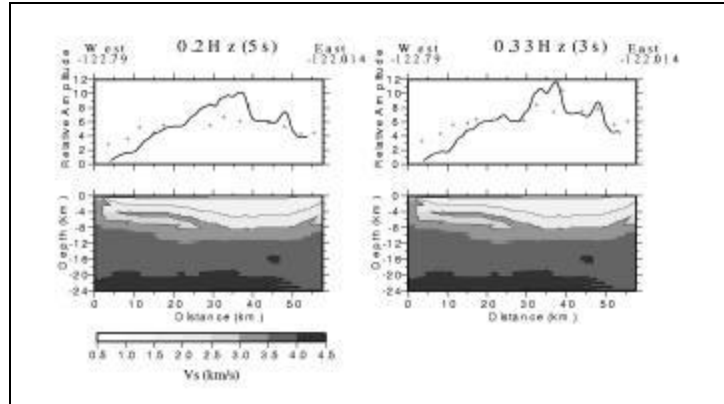


**Figure 7. Spectral amplitudes relative to a rock site indicated in Figure 6, calculated at specific frequencies shown on top of each panel. Top panels. Comparison of relative spectral amplitudes using synthetic seismograms from the Nisqually earthquake (solid line) and recorded round motion from the Chi-chi, Taiwan earthquake (crosses) (Pratt et al., 2003) along the E-W line shown in Figure 1. Bottom panels. Top 24km of the vertical cross-section of the 3D velocity model along the E-W line**

## CONCLUSIONS

In this study we show results of validation analyses of a velocity model for 3D long-period ground motion simulations in the Puget Sound region. Our simulation of ground motion from the Nisqually earthquake suggests that the regional tomographic velocity model of Parsons et al. [1], combined with the Seattle basin basement geometry proposed by Blakely [2], and N-S and E-W basin structure cross-sections from the SHIPS experiments provide very good information that is essential for developing efficient velocity models of the Seattle region for 3D simulations. Our velocity model performs well in reproducing basin structural effects on long period ground motion from the Nisqually earthquake in the Seattle basin. The analyses of our simulation results indicate that waves with periods longer than 3 sec are mainly affected by the deep geological structure of the Seattle basin. As pointed out by Frankel et al. [7], future improvements of the velocity models for 3D simulations need to be focussed on the shallow structure of the basins in the Puget Sound region. These improvements should be guided by modeling observed ground motion data for several seismic sources at periods shorter than 2 sec (e.g. Pratt et al. [11]).

## REFERENCES

1. Parsons T, Blakely RJ, Brocher TM. "A simple algorithm for sequentially incorporating gravity observations in seismic travelttime tomography". *International Geology Review* 2001; 43: 1073-1086.
2. Blakely RJ, Wells RE, Weaver CS. "Puget sound aeromagnetic maps and data". U.S. Geological Survey Open-File Report 1999; 99-514, <http://geopubs.wr.usgs.gov/open-file/of99-514>.
3. Brocher TM, Parsons T, Creager KC, Crosson RS, Symons NP, Spence G, Zelt BC, Hammer PTC, Hyndman RD, Mosher DC, Trehu AM, Miller KC, Brink US, Fisher MA, Pratt TL, Alvarez MG, Beaudoin BC, and Weaver CS. "Wide-angle seismic recordings from the 1998 Seismic Hazards Investigation in Puget Sound (SHIPS), western Washington and British Columbia". U.S. Geological Survey Open-File Report 1999; 99-314: 110p.
4. Brocher TM, Parsons T, Blakely RJ, Christensen NI, Fisher MA, Wells RE, SHIPS Working Group. "Upper crustal structure in Puget Lowland, Washington: Results from the 1998 Seismic Hazards Investigation in Puget Sound". *J. Geoph. Res.* 2001; 106: 13,541-13,564.
5. Calvert AJ, Fisher MA, SHIPS Working Group. "Imaging the Seattle fault zone with high-resolution seismic tomography". *Geoph. Res. Lett* 2001; 28: 2337-2340.
6. Van Wagoner TM, Crosson RS, Creager KC, Medema G, Preston LA, Symons NP, Brocher TM. "Crustal structure and relocated earthquakes in the Puget Lowland, Washington, from high-resolution seismic tomography". *J. Geoph. Res.* 2002; 107(B12):2831,doi:10.10129/2001JB000710.
7. Frankel A, Stephenson W. "Three-dimensional simulations of ground motions in the Seattle region for earthquakes in the Seattle fault zone". *Bull. Seism. Soc. Am.* 2000; 90: 1251-1267.
8. Frankel A, Carver C, Cranswick E, Meremonte M, Bice T, Overturf D. "Site response for Seattle and source parameters of earthquakes in the Puget Sound region". *Bull. Seism. Soc. Am.* 1999; 89: 468-483.
9. Hartzell S, Carver D, Cranswick E, Frankel A. "Variability of Site response in Seattle, Washington". *Bull. Seism. Soc. Am.* 2000; 90: 1237-1250.
10. Frankel A, Carver D, Williams RA. "Nonlinear and linear site response and basin effects in Seattle for the M6.8 Nisqually, Washington, earthquake". *Bull. Seism. Soc. Am.* 2000; 92: 2090-2109.
11. Pratt TL, Brocher TM, Weaver CS, Creager KC, Snelson CM, Crosson RS, Miller KC, Trehu AM. "Amplification of seismic waves by the Seattle basin, Washington state". *Bull. Seism. Soc. Am.* 2003; 93: 533-545.

12. Finn CA, Philips WM, Williams DL. "Gravity anomaly and terrain maps of Washington". U.S. Geological Survey, Geophysical Investigation Map 1991; GP-988.
13. Johnson SY, Dadisman SV, Childs J, Stanley WD. "Active tectonics of the Seattle Fault and cross-cutting strike-slip faults in the central Puget Sound Lowlands, Washington: implications for earthquake hazards". *Geol. Soc. Am. Bull.* 1999: 1042-1053.
14. Pratt TL, Johnson S, Potter C, Stephenson W, Finn C. "Seismic reflection images beneath Puget Sound, western Washington state: the Puget Lowland thrust sheet hypothesis". *Journ. Geoph. Res.* 1997; 102: 27,469-27489.
15. Crosson RS. "Crustal structure modeling of earthquake data. Velocity structure of the Puget Sound region, Washington". *J. Geophys. Res.* 1976; 81: 3047-3054.
16. Graves R "Simulating seismic wave propagation in 3D elastic media using staggered grid finite differences". *Bull. Seism. Soc. Am.* 1996;86:1091-1106.
17. Miller K.C Snelson CM. "Structure and geometry of the Seattle basin, Washington state- results from Dry SHIPS'99: Collaborative research (USGS, OSU, UTEP), Progress Report to USGS,2001.
18. Yount JC, Dembroff GR, Barats GR. "Map showing depth to bedrock in the Seattle 30' by 60' quadrangle, Washington, U.S. Geological Survey, Miscellaneous Field Studies Map, MF-1692, scale 1:100,000", 1985.
19. Hall JB, Othberg KL. "Thickness of unconsolidated sediments, Puget Lowland, Washington, State of Washington, Department of Natural Resources, Geologic Map GM-12, Washington", 1974.
20. Brocher TM, Parsons T, Trehu AM, Snelson CM, Fisher MA. "Seismic evidence for widespread serpentinized forearc upper mantle along the Cascadia margin". *Geology* 2003; 31, 3: 267-270.
21. Ichinose GA, Thio HK, Somerville PG. "Rupture process and near-source shaking of the 1965 Seattle-Tacoma and 2001 Nisqually, intraslab earthquakes". *Geophys. Res. Lett.* 2003 (submitted).
22. Pitarka A. "3D elastic finite-difference modeling of seismic wave propagation using staggered-grid with non-uniform spacing", *Bull. Seism. Soc. Am.* 1999; **89**: 54-68.
23. Pitarka A, Irikura K. "Basin structure effects on long period strong ground motions in the San Fernando valley and the Los Angeles Basin from the 1994 Northridge earthquake and an aftershock", *Bull. Seism. Soc. Am.* 1996; 86:S126-S137.